JOURNAL OF MATERIALS SCIENCE 31 (1996) 617–623

Structure and ferroelectric properties dependence on thermal treatment of modified lead titanate thin films

J. MENDIOLA, M. L. CALZADA, R. SIRERA, P. RAMOS
Instituto de Ciencia de Materiales de Madrid (C.S.I.C) Serrano, 144, 28 006 Madrid, Spain

Calcium modified lead titanate thin films have been prepared from a sol–gel method. Different thermal conditions have been used for the crystallization of the as-deposited amorphous films. The influence of thermal treatment on the perovskite structure and strain of the films is studied by a grazing incidence X-ray diffraction technique (GIXRD). The ferroelectric response of the films is related to their crystalline structure and chemical composition.

1. Introduction

Ferroelectric thin films based on modified lead titanate compositions are of increasing interest for their possible applications in non-volatile ferroelectric memories, surface acoustic wave (SAW) devices, actuators, infrared (I.R.) detectors, etc., [1, 2].

Among the deposition techniques currently used to produce high quality ferroelectric thin films, the sol–gel process has the advantage of providing good homogeneity, ease of compositional control and low temperature processing [3]. In sol–gel processing, crystallization proceeds from amorphous structures after thermal treatment. Development of perovskite phase in these films, depends upon the solution chemistry and thermal treatment used. Rapid thermal annealing (RTA) has been used to maximize the content of perovskite phase by circumventing the temperature range in which pyrochlore phases are stable, to avoid reactions between the bottom electrode and the ferroelectric layer and to prevent evaporation of PbO. These defects (second phases, substrate–ferroelectric interfaces, lead and oxygen vacancies, etc.) restrict many applications of ferroelectric films. Thus, a complete crystallographic characterization which shows the distribution of ferroelectric and non-ferroelectric phases in the polycrystalline films is desired [4]. From this knowledge, an approach for modelling electric properties of films should be possible.

The conventional $\theta-2\theta$ X-ray powder diffraction method is not suitable for analysing polycrystalline thin films, since the incident beam penetrates into the substrate and information, not only of the polycrystalline layer but also of the substrate itself is obtained. Instead of this, a grazing incident X-ray diffraction (GIXRD) technique has been proved recently to be more feasible for this type of sample [5, 6].

In this work, the GIXRD is used to obtain depth profiles of the phase compositions and residual strains in $Ca_xPb_{1-x}TiO_3$ sol–gel derived films crystallized with different thermal treatments. Electric characterization is also carried out in these films and correlations between these results and those obtained from the GIXRD technique, are attempted.

2. Experimental procedure

2.1. Thin film preparation

For the synthesis of calcium modified lead titanate precursor solutions (Fig. 1), a lead and titanium sol was first prepared by reacting titanium di-isopropoxide bis-acetylacetonate, $Ti(OC_3H_7)_2(CH_3COCHCOCH_3)_2$, and trihydrated lead acetate, $Pb(CH_3COO)_2.3H_2O$, in 1,3-propanediol solvent, $HO(CH_2)_3OH$ [7]. Molar ratios of 5:1 and 0.76:1 were used for diol:solvent and lead:titanium, respectively. A water-dissolved calcium acetate, $Ca(CH_3COO)_2$, with a 5:1 molar ratio of water to diol and a 0.24:1 molar ratio of calcium to titanium, was added to the former sol. After vigorous stirring, a stable solution with ≈ 0.9 M concentration and $Pb_{0.76}Ca_{0.24}TiO_3$ nominal composition was obtained [8].

The precursor solution was deposited on Pt–TiO_2–SiO_2–(1 0 0) Si substrates by spin-on at 2000 r.p.m. for 45 s. These samples were heated at 350 °C for 60 s on a hot plate for solvent removal and partial organic pyrolysis. To achieve crystallization in the films, different thermal treatments were tested. These treatments consisted of heating at 5 and 40 °C min^{-1} up to 650 °C with a soaking time of 12 min, and the rapid heat treatment consisted of bringing the furnace to the desired temperature (650 °C) and stabilizing it, putting the film in it, maintaining the temperature for 12 min, and air-quenching to room temperature. Thicknesses of about 500 nm and an average grain size for the former samples of 100, 70 and 20 nm, respectively, have been obtained (Fig. 2).

0022–2461

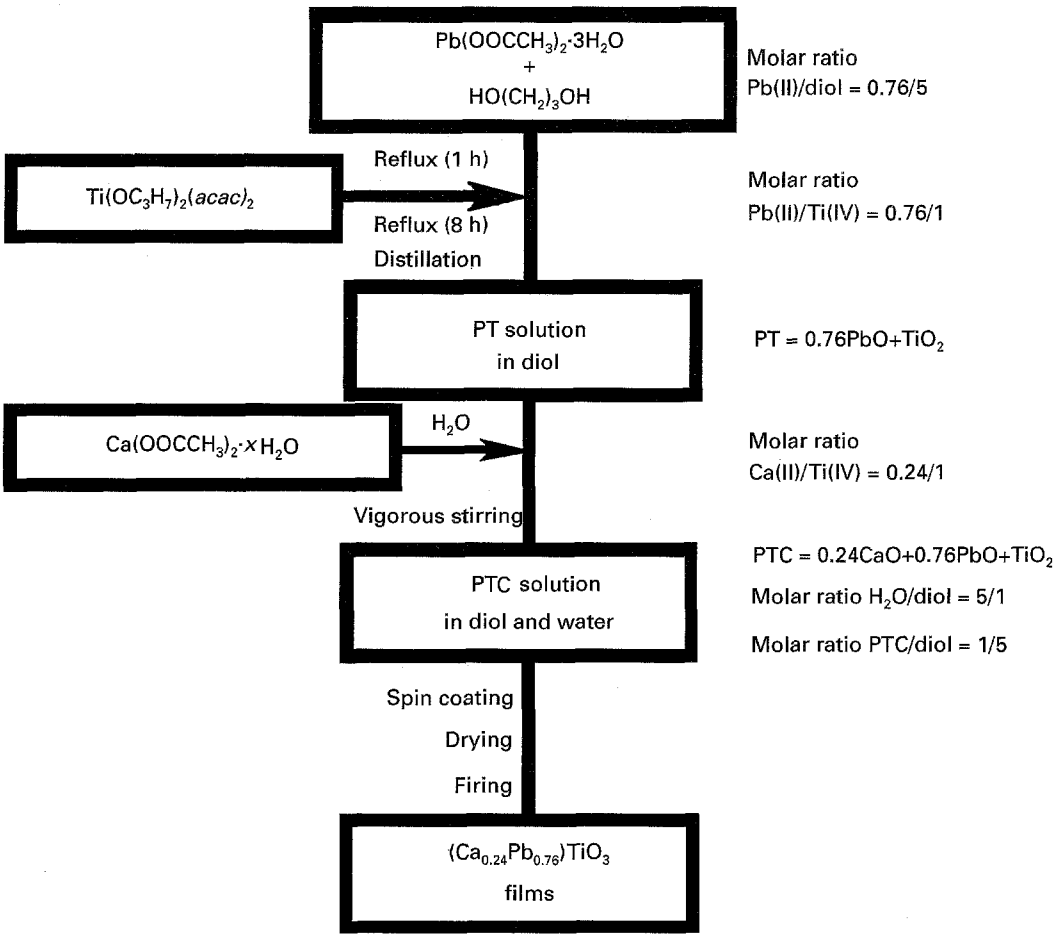

Figure 1 Preparation scheme of the films.

2.2. X-ray diffraction measurements

The grazing incidence X-ray asymmetric Bragg geometry used for the analysis of the ferroelectric thin films is schematically shown in Fig. 3.

XRD data were collected on a Siemens D 500 powder diffractometer with uncoupled $\theta-2\theta$, 0.1° divergent incident slit, a special 0.4° axial Soller slit and a flat LiF monochromator in the diffracted beam. A Cu anode operating at 40 kV and 25 mA and a scanning speed of 0.15° min^{-1}, were used.

As the grazing incidence angle, α, increases, the diffracting volume also increases according to $\sin\alpha \approx \alpha$ and, thus, a deeper layer of the sample can be analysed. All the recorded data allow one to obtain information about the profile of the films.

Fig. 4 shows the 2θ scans of samples annealed with the three types of thermal treatments tested in this work.

1. a slow heating rate of 5 °C min^{-1}, hereinafter called sample A;
2. a moderated heating rate of 40 °C min^{-1}, hereinafter called sample B; and
3. a rapid heating, hereafter called sample C.

The patterns were obtained with a grazing incidence angle of $\alpha = 1°$. In these patterns, not only the perovskite diffraction peaks are observed but also other peaks corresponding to Laue reflections of the (1 0 0) silicon substrate [9] and to pyrochlore phases ($PbTi_3O_3$, $Pb_2Ti_2O_6$ and $PbTi_2O_7$). These phases are always present in films annealed with slow heating rates.

In order to obtain depth profile information through the thickness of the ferroelectric films, a sequential set of scans was performed measuring the 0 0 1 and 1 0 0 profiles from $\alpha = 1$ to 3° with 0.5° steps.

The recorded data were corrected by background, K_{α_2}, stripping and smoothing. An angular shift

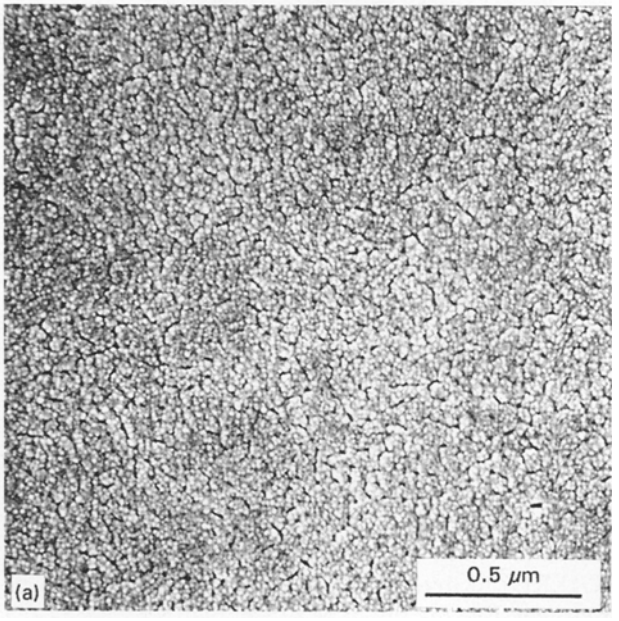

Figure 2 Scanning electron micrographs of the three samples follwing heat treatment: (a) "rapid", (b) 40 °C min^{-1}, and (c) 5 °C min^{-1}.

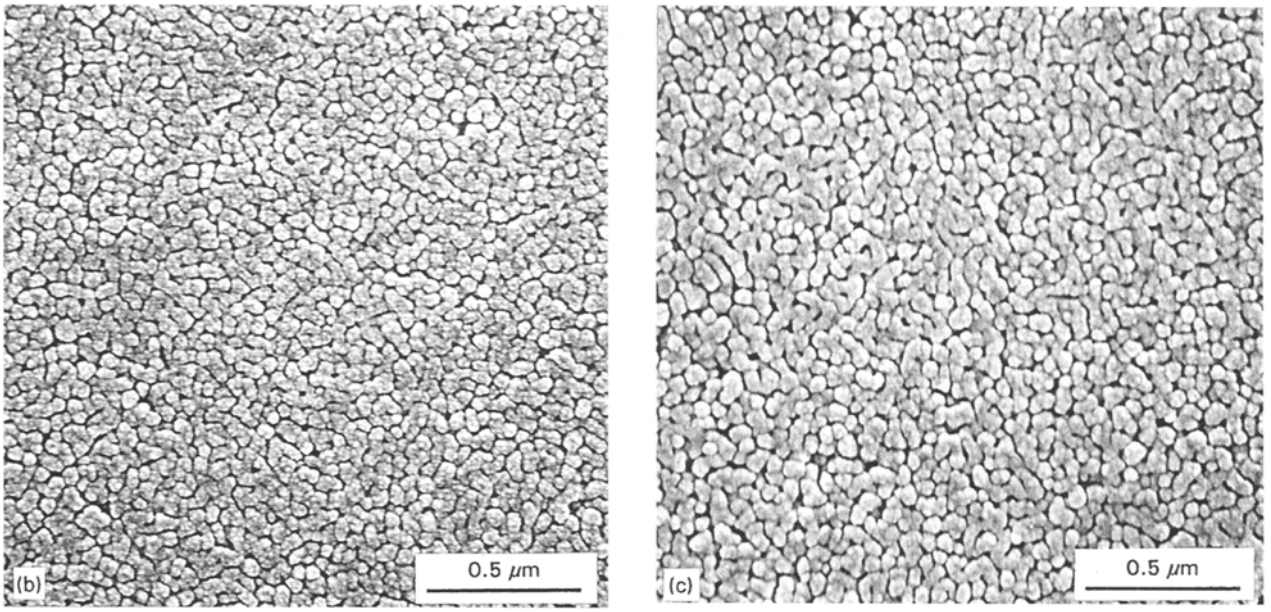

Figure 2 (Continued)

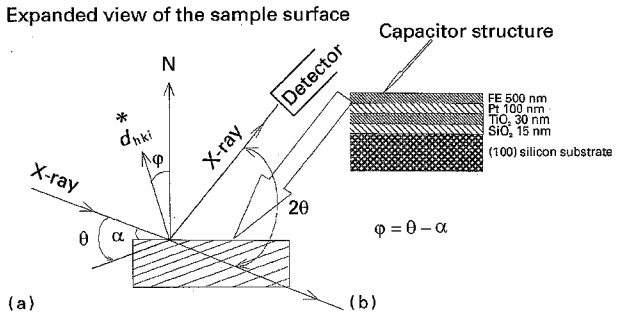

Figure 3 Schematic diagram of the GIXRD technique:(a) expanded view of the sample surface, and (b) capacitor structure.

correction due to the X-ray refraction was applied [10], according to the equation

$$\Delta 2\theta \approx \alpha - (\alpha^2 - \alpha_c^2)^{1/2}$$

The expression $\alpha_c \approx 16 \times 10^{-4} \rho^{1/2} \lambda$ is used to calculate the critical angle for a total reflection, considering a density of $\rho \approx 6.5$ g cm^{-3}, since films seem to show a lower dense microstructure than ceramics, as can be observed in the SEM micrographs of Fig. 2. Figure 5 shows the profile results obtained for the films after deconvolution of the 0 0 1 and 1 0 0 peaks with commercial software. Note that overlapping of the film profiles increases

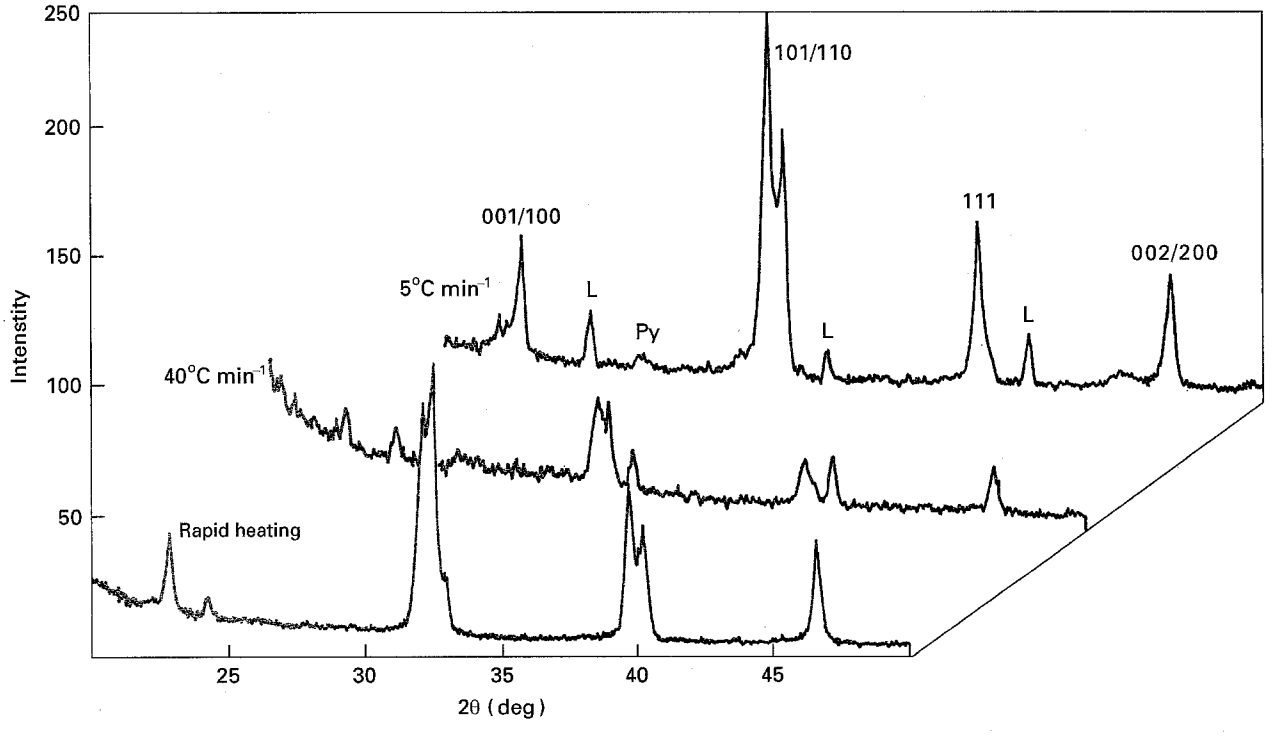

Figure 4 GIXRD patterns (α = 1°) of the three types of samples, have reflection of Si; Py, pyrochlore peaks.

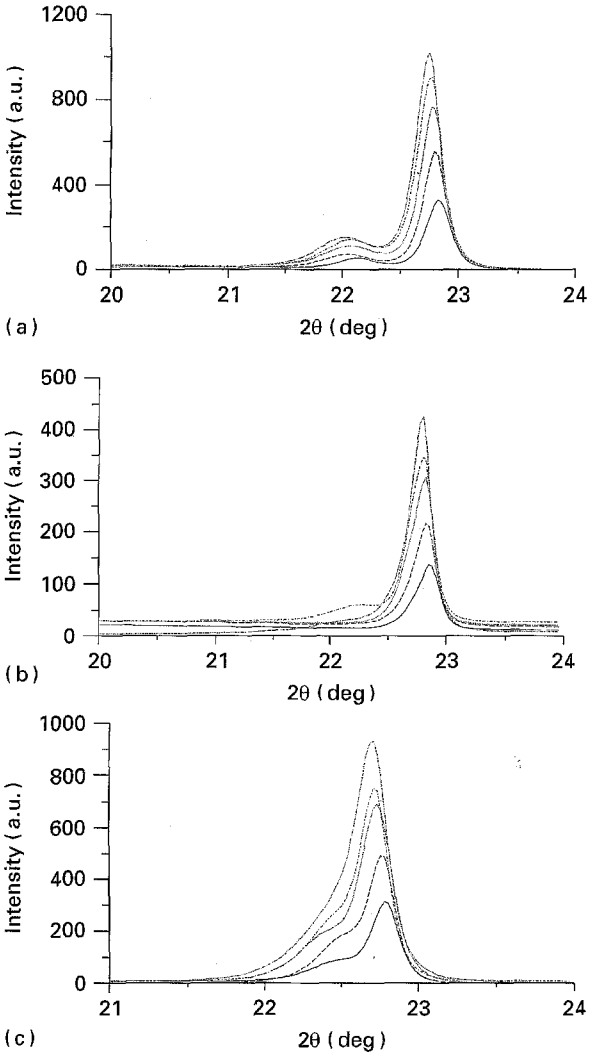

Figure 5 GIXRD scans of the three samples, A-C, at (a) 5 °C min^{-1}, (b) 40 °C min^{-1}, (c) rapid heating respectively. Incident beam angle, α°:(—11.0°, (– – –) 1.5°, (.....) 2.0°, (.. .. ..) 2.5°, (.. .. .. ..) 3.0°.

with the increasing heating rate of the thermal treatment used.

The corrected and fitted profiles allowed are to calculate the cell parameters and their variation with depth. Strains were deduced using a line broadening analysis, as will be shown later on.

2.3. Electrical characterization

2.3.1. Hysteresis loops

To carry out the electrical measurements, Pt dot electrodes of 2 mm diameter were deposited by sputtering on the top surface of the films. Hysteresis loops were performed using a modified Sawyer tower circuit. A sinusoidal signal of variable amplitude and 1 Hz frequency was used. Resistance (R) and capacitance (C) compensation was realized using a previous measurement of R and C with a low and non-disturbative voltage. Figure 6 shows the hysteresis loops and the current versus the applied electric field for the three types of samples.

2.3.2. Switching currents

A sequence of square pulses was applied to measure the current curves as is depicted in Fig. 7. After several

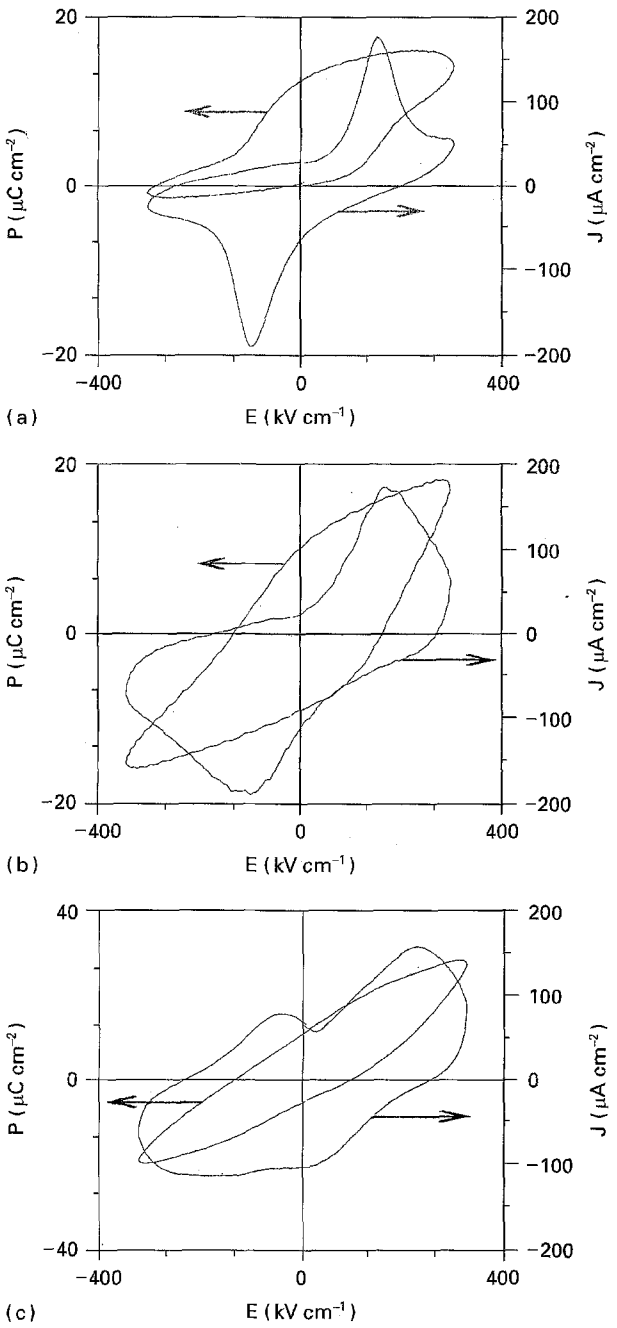

Figure 6 Hysteresis and current curves of the samples. (a) Sample A, 5 °C min^{-1}: + Ec =150 kV cm^{-1}, −Ec = −95 kV cm^{-1}, $2P_R$ =12.3 μC cm^{-2}. (b) Sample B, 40 °C min^{-1}: + Ec = 184 kV cm^{-1}, − Ec =120 kV cm^{-1}, $2P_R$ =19.5 μC cm^{-2}. (c) Sample C, rapid heating: + Ec = 226 kV cm^{-1}, − Ec = −165 kV cm^{-1}, $2P_R$ = 13.6 μC cm^{-2}. Where Ec = Coercive field

polarization pulses of 16 V amplitude and 200 μs width, with an interval of 20 μs, two equal pulses of opposite sign were used for the measurement of the current curves. Then, the net poling charge (non-linear ferroelectric charge) and switching time were obtained. Figure 8 shows the switching current curves.

3. Results and discussion

It has been reported previously [11], that so-called rapid thermal annealing (RTA) avoids the formation of pyrochlore phases in lead titanate based materials. Although, the annealing conditions tested in this work for film crystallization are not those reported for RTA,

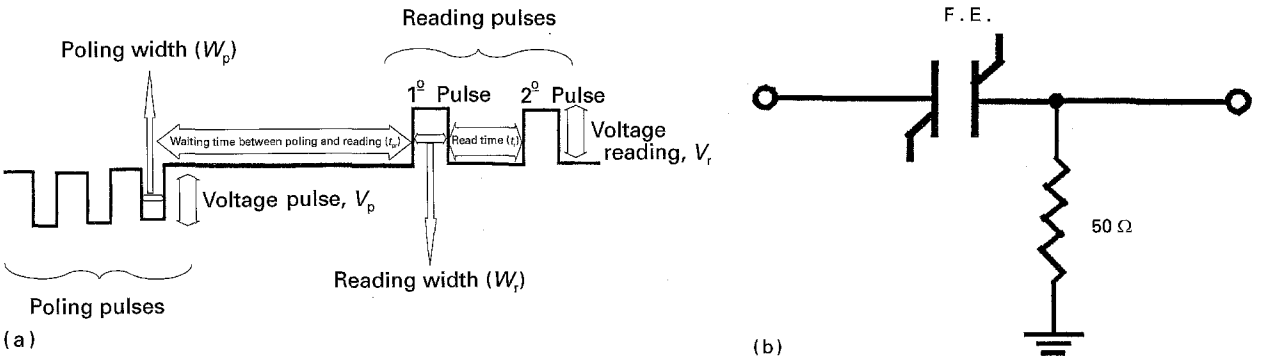

Figure 7 (a) Pulse sequence, and (b) schematic circuit for switching measurements.

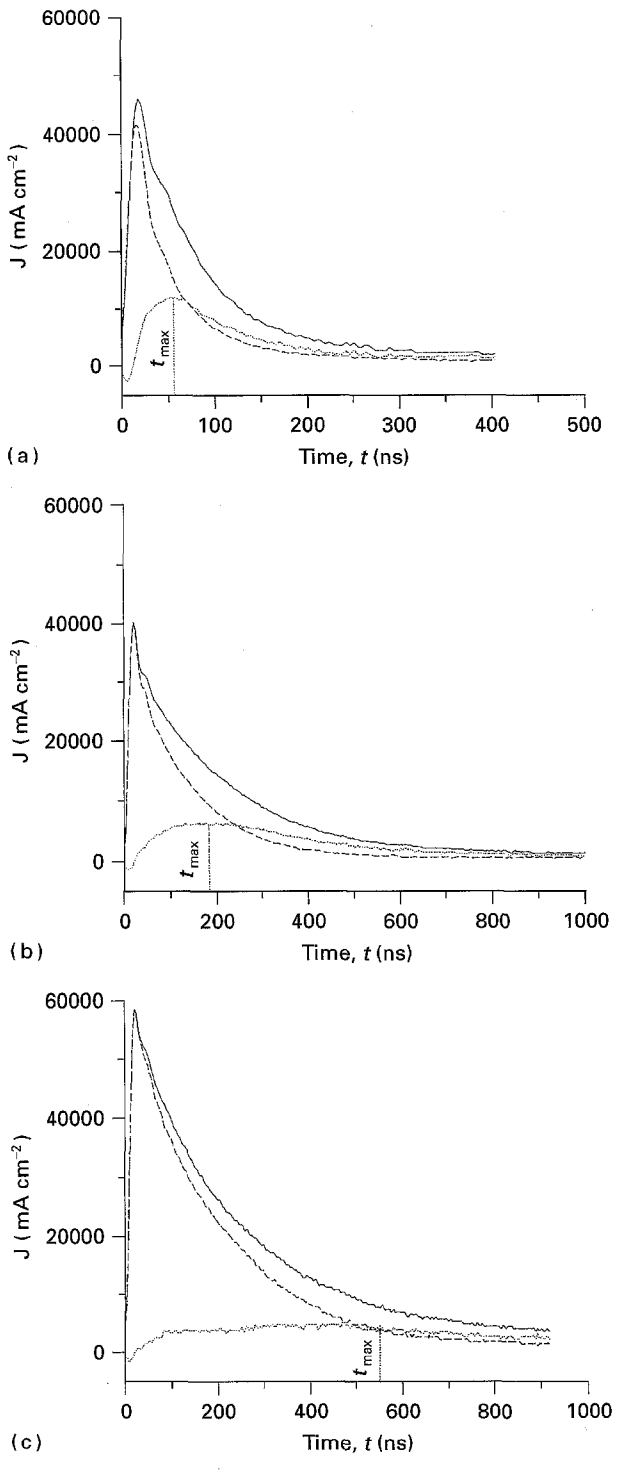

Figure 8 Switching current curves for samples:(a) A, 5 °C min^{-1}, (b) B, 40 °C min^{-1}, and (c) C, rapid heating, following:(—) 1°, (– – – –) 2°, (.....) 1–2° pulses.

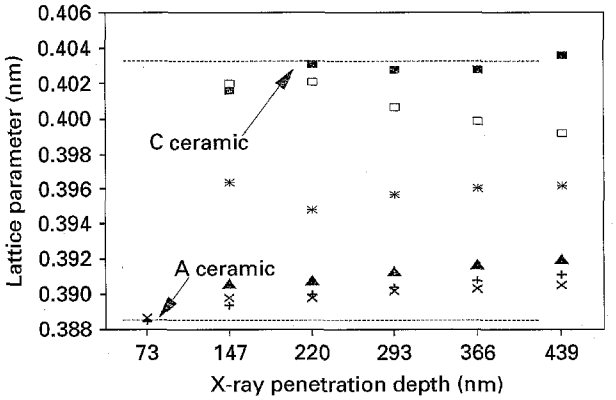

Figure 9 Lattice parameter variation versus X-ray penetration depth:(■) c5C, (+) a5C, (*) crp, (□) c 4OC, (×) a 4OC, (▲) arp. Where c5C is c-axis of sample A (heating rate of 5 °C min^{-1}), a5C is a-axis of sample A (heating rate of 5 °C min^{-1}), crp is c-axis of sample C c4OC is c-axis of sample B (heating rate of 40 °C min^{-1}) a4OC is a-axis of sample B (heating rate of 40 °C min^{-1}) arp is a-axis of sample C (rapid heating rate).

it is observed that an increase in heating rate leads to a decrease of pyrochlore phases in the films. However, perovskite distortion is always smaller in samples treated with rapid heating rates. Figure 9 shows that the cell parameters of sample A are closer to those of bulk ceramics with the same composition, than the parameters of the other two samples, B and C. In this figure, variation of the a and c cell parameters, as a function of penetration depth of the X-ray beam, can be observed. Penetration of the beam is calculated for each grazing angle, considering an attenuation of $I/I_0 = 1\,e^{-1}$ and taking into account the formula

$$I/I_0 = \exp^{-\mu t[1/\sin\alpha + 1/\sin(2\theta - \alpha)]}$$

where μ is the linear absorption, t the thickness, α the grazing incident angle and 2θ the diffraction angle. This figure shows a larger variation and lower values for the c-axis in sample B than in samples A and C. These phenomena can be due to variation in chemical composition through the film thickness and/or to strain effects induced by the substrate.

After deconvolution of the overlapped 001/100 peaks, large broadening is observed in both peaks, specially in the 001 peak. This effect could be explained considering a mixture of perovskite compositions with different amounts of Ca, since the c parameter of the perovskite is very sensitive to this type of variation, meanwhile the a-axis remains almost constant. This effect has been observed also in ceramics

[12], for other modified lead titanate compositions. Recently, Qu *et al.* [13] have reported broadening even in pure lead titanate films. Therefore, the broadening effect that is observed in the films cannot be imputed only to composition inhomogeneities, but also to other causes.

To perform the profile analysis in the films, some previous considerations have had to be made, to simplify the calculation. The broadening contribution of grain size in samples A and B has been neglected since it is close to 100 nm. Thus, strains only have been considered in the profile analysis. In these cases, integral breadths are obtained and corrected by instrumental contribution, using a standard ceramic with a large grain size. The conventional integral breadth method is thus applied [14], considering the expressions

$$\beta = (B_{exp}^2 - B_{st}^2)^{1/2}$$

$$\varepsilon(\%) = \beta/4tan\theta$$

where B_{exp} and B_{st} are the breadths of the experimental and the standard samples, and ε the strain. For sample **C**, since the grain size is much smaller, its contribution to the broadening cannot be neglected and, in this case, the variance method [15] is more appropriate for calculation of strains along [0 0 1]. In this film, the following expression is used

$$< \varepsilon^2 > = (W_{oc}/4tg^2\theta) \times \pi/180$$

where W_{oc} is the intercept of the variance-range curve, after all the corrections have been performed.

Fig. 10 shows strain variation with X-ray penetration depth. Note how large the strain is along the [0 0 1] direction, compared with the [1 0 0] direction. These results are similar to those obtained for bulk ceramics where the 0 0 1 profile is also very broad [12]. By considering the former results, a larger global strain is deduced for samples A and B than for sample C, mainly along the [0 0 1] direction.

The GIXRD method used in this work does not supply information for each separated volume layer of film, since for each grazing angle, α, the information also includes one of the previous layers. However, even considering this limitation, the information obtained with this technique is very useful compared with conventional $\theta-2\theta$ XRD, where interference of the substrate cannot be avoided.

According to the results obtained from GIXRD analysis, it can be said that films annealed with rapid heating show lower content of pyrochlore phases than films prepared with slow heating. Besides the strain induced by the substrate on the cell structure of the perovskite, crystallinity is always lower in films prepared by rapid heating than with slow heating.

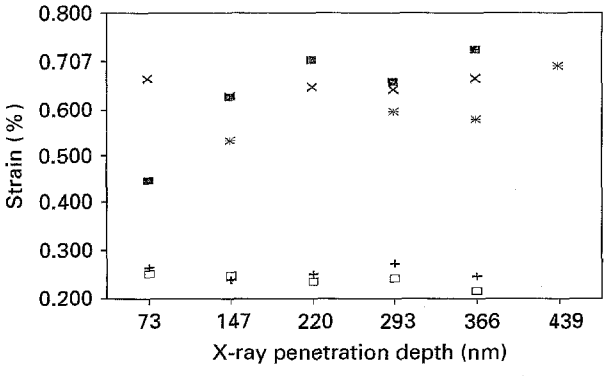

Figure 10 Lattice strain variation with X-ray penetration depth.

An average strain value of 4.0×10^{-3} has been reported previously [12] for modified lead titanate bulk ceramics. Since the values obtained here for samples A and B are 6.8×10^{-3}, disagreement between both values has to be ascribed to the special nature of the films. Nevertheless, the *c* parameters deduced from the average strain of the films are slightly larger than the parameters experimentally obtained, indicating the existence of lead and oxygen vacancies produced by small volatilization of PbO during thermal treatment. For sample C, after the appropriate corrections, the intrinsic strain of the film is 2×10^{-3}. The average *c* parameter deduced from this strain is much smaller than that of the other two samples. Thus, the presence of an amorphous phase not crystallized during heating is suggested, since such large quantities of PbO losses are not possible.

The Fig. 6 shows a better defined hysteresis loop and a lower value of the coercive field for sample A than for sample B, although (remanent polarization) $2P_R$ is smaller in the first case. For sample C, the large non-ferroelectric current masks the true hysteresis loop. Switching curves are also different. For all samples, application for a short time of an electric field previous to poling (de-ageing), favours reorientation of domains. For sample **B**, the increase of time elapsed between the electric treatment and the switching measure, leads to a decrease of the charge implied (Table I), this decrease for samples **A** and **C** being much more rapid.

The variation of switching time, τ, defined as double the time for the maximum current, is also remarkable. For sample A, τ is about 100 ns; whereas for sample B, τ moves from 400 ns, just after electric treatment, to 140 ns, 30 min after. This increase of switching associated with domain wall mobility, will probably have been caused by rearrangement of a space charge moving from the ferroelectric layer to the ferroelectric–electrode interface.

The lack of squareness in the hysteresis loops of samples A and B can be associated, according to Mihara *et al.* [16], to the microstructure dependent internal space charge; the smaller the grain size, the larger the space charge. Therefore, since the squareness of sample **B** is less than that of sample **A**, a larger space charge has to be present in the former than in

TABLE I Variation of the switching parameters with elapsed time between the previous electrical treatment and measure (■)c5C, (+)a5C, (*)crp, (□)a40C, (×)c40C.

Time, *t*, elapsed (seg)		$P(\mu C\ cm^{-2})$		t_{max}(ns)	
40 °C min^{-1}	Rapid	40 °C min^{-1}	Rapid	40 °C min^{-1}	Rapid
0.3	0.3	3.298	3.110	200	472
1.0	2.5	2.463	2.433	136	88
6.0	6.0	2.151	1.464	128	100
10.0	8.0	1.634	1.226	88	112
30.0	16.0	1.178	0.732	72	84

the later. This result is in accordance with that deduced from the grain size of each sample. On the other hand, the space charge of the samples produces an internal bias field which causes the shift of the hysteresis curves shown in Fig. 6.

4. Conclusions

According to the experimental results of this work, an increase in the thermal treatment heating rate used for the crystallization of sol–gel derived films, facilitates the formation of a single perovskite phase.

Together with the perovskite phase, second pyrochlore phases are observed in films prepared by slow heating. Formation of a large space charge due to PbO losses is also detected in these films. However, the films crystallized with rapid heating do not present pyrochlore phases and have low space charge, although some amorphous phase remains in these films after crystallization.

Thermal treatment causes a compressive strain in the films which becomes larger closer to the substrate. This strain seems to produce an increase in the coercive field of the ferroelectric films.

During poling, a rearrangement of the space charge of the films is produced. Therefore, the way of poling affects the electric results obtained from these films.

Due to space charge, related to the thermal treatment of the films, more studies about the kinetics of the solid state reactions which occur in each type of films need to be made.

Acknowledgements

This work has been supported by Spanish Projects MAT91-422 (CICYT) and C120/91 (CAM), and has been declared of technological interest by the European Action COST514.

References

1. J. F. SCOTT, C. A. PAZ ARAUJO and L. D. MACMILLAN, *Condensed Matter News* **1** (1992) 16.
2. R. WATTON, *Integrated Ferroelectrics* **4** (1994) 175.
3. Y. XU and J. D. MACKENZIE, *ibid.* **1** (1992) 17.
4. D. M. TAHAN and A. SAFARI, Proceedings of the Eighth Institute of Electrical Engineers International Symposium on Applications of Ferroelectrics (Greenville, 1992) p. 420.
5. T. C. HUANG, *Adv. in X-ray Anal.* **33** (1991) 91.
6. R. P. GOEHNER and M. O. EATOUGH, *Powder Diffraction* **7** (1992) 2.
7. N. J. PHILLIPS, M. L. CALZADA and S. J. MILNE, *J. Non-Cryst. Solids* **147–148** (1992) 285.
8. R. SIRERA, M. L. CALZADA, F. CARMONA and B. JIMENEZ, *J. Mater. Sci. Lett.* **13** (1994) 1804.
9. R. A. VAIA, M. S. WEATHERS and W. A. BASSETT, *Powder Diffraction* **7** (1994) 44.
10. T. TAKAYAMA and Y. MATSUMOTO, *Adv. in X-ray Anal.* **33** (1990) 109.
11. L. SHI, S. B. KRUPANIDHI and G. H. HAERTLING, *Integrated Ferroelectrics* **1** (1992) 111.
12. G. F. FU, L. PARDO and J. MENDIOLA, in Proceedings of the Third European Ceramics Society Meeting Vol. II (Madrid, 1993), pp. 157–162.
13. B. QU, D. KONG, W. ZHONG, P. ZHANG and Z. WANG, *Ferroelectrics* **145** (1993) 39.
14. M. P. KLUG and L. E. ALEXANDRE, "X-ray Diffraction Procedures", (Wiley, New York, 1974) p. 661.
15. J. I. LANGFORD and A. J. C. WILSON, in "Crystallographic and Crystal Perfection", edited by G. N. Ramachandran (Academic Press, New York, 1963) pp. 207–222.
16. T. MIHARA, H. WATANABE, H. YOSHIMORI, C. A. PAZ DE ARAUJO, B. MELNICK and L. D. MCMILLAN, *Integrated Ferroelectrics* **1** (1992) 269.

Received 31 October 1994
and accepted 7 June 1995